

A first-order dynamical model of hierarchical triple stars and its application *

Xing-Bo Xu^{1,2}, Fang Xia¹ and Yan-Ning Fu¹

¹ Purple Mountain Observatory, Chinese Academy of Sciences, Nanjing 210008, China;
xbxu@pmo.ac.cn; xf@pmo.ac.cn

² University of Chinese Academy of Sciences, Beijing 100049, China

Abstract For most hierarchical triple stars, the classical double two-body model of zeroth-order cannot describe the motions of the components under the current observational accuracy. In this paper, Marchal’s first-order analytical solution is implemented and a more efficient simplified version is applied to real triple stars. The results show that, for most triple stars, the proposed first-order model is preferable to the zeroth-order model both in fitting observational data and in predicting component positions.

Key words: celestial mechanics — binaries: general — stars: kinematics and dynamics — methods: analytical

1 INTRODUCTION

A hierarchical triple star is composed of a close binary and a distant third component. About one thousand stars of this kind are contained in the latest on-line version of *The Multiple Star Catalog* (Tokovinin 1997). In these systems, the primary components are usually bright. Bright stars are useful in many aspects (e.g. Urban & Seidelmann 2014). Though a set of isotropic and dense stars is crucial for some applications such as navigation, the stars with nearby companions are usually excluded. This is the case for the Hipparcos Celestial Reference Frame, as recommended in IAU resolution B1 (2000)¹. For triple stars, the problem lies mainly in that the primary positions generally cannot be predicted accurately by the almost exclusively used model, namely the classical double two-body model.

Hierarchical triple stars are also of great interest in stellar physics and galactic astronomy, due to the fact that their dynamical evolution is important to both stellar and galactic evolutions (e.g. Binney & Merrifield 1998, Valtonen & Karttunen 2006, Aarseth 2003). Moreover, these systems are often studied in terms of stability of the general three-body problem (e.g. Marchal & Bozis 1982, Li, Fu & Sun 2009). In some case studies, the results are sensitive to the mass parameters and the initial conditions (e.g. Orlov & Zhuchkov 2005), the accuracies of which are limited again by the double two-body model used in fitting observations (e.g. Liu et al. 2009).

As a zeroth-order solution of the hierarchical three-body problem, the double two-body model has the advantage of being analytical and simple. The existing first-order analytical solutions are more accurate. The former one is still dominantly used, while the latter ones, as far as we know, remain little used in fitting observations. In this paper, the first-order solution by Marchal is efficiently implemented. This is achieved mainly by making some simplified modifications and high order approximations to

* This research is supported by the National Natural Science Foundation of China under Grant Nos. 11178006 and 11203086.

¹ http://www.iau.org/static/resolutions/IAU2000_French.pdf

Marchal's solution. In the context of fitting observations of triple stars, we call Marchal's solution and the double two-body solution, respectively, the M-model and the K-model.

In section 2, the M-model is implemented. In section 3, the improvement in accuracy of M-model to K-model is statistically discussed with a set of sampling triple stars. In section 4, a simplified M-model is given and applied to real triple stars. Concluding remarks are given in the last section.

2 AN IMPLEMENTATION OF M-MODEL

Consider a hierarchical three-body problem in an inertial coordinate system $\{O-xyz\}$, where O is the center of mass and the z -axis parallel to the total angular momentum C . Denoting the masses of the inner two bodies by m_1 and m_2 , and the mass of the third body by m_3 , we will use the following mass-dependent parameters,

$$\begin{aligned} m_t &= m_1 + m_2 + m_3, & m_i &= \frac{m_1 m_2}{m_1 + m_2}, & m_o &= \frac{(m_1 + m_2) m_3}{m_t}, \\ \beta_i &= \frac{G^2 m_1^3 m_2^3}{m_1 + m_2}, & \beta_o &= \frac{G^2 (m_1 + m_2)^3 m_3^3}{m_t}, & \beta_1 &= \frac{G^2 (m_1 + m_2)^7 m_3^7}{(m_1 m_2 m_t)^3}, \end{aligned}$$

where G is the gravitational constant. Let \mathbf{r} be the position vector of m_2 relative to m_1 , and \mathbf{R} the position vector of m_3 relative to the center of mass of the binary. The ratio $\varepsilon = \frac{r}{R} \equiv \frac{|\mathbf{r}|}{|\mathbf{R}|}$ is a small quantity.

The Delaunay variables as expressed in terms of the ordinary orbital elements $(a, e, i, \omega, \Omega, M)$ are

$$\begin{aligned} \mathcal{L}_i &= m_i \sqrt{G(m_1 + m_2) a_i}, & \mathcal{G}_i &= \mathcal{L}_i \sqrt{1 - e_i^2}, & \mathcal{H}_i &= \mathcal{G}_i \cos i_i, \\ \ell_i &= M_i, & g_i &= \omega_i, & h_i &= \Omega_i, \\ \mathcal{L}_o &= m_o \sqrt{G m_t a_o}, & \mathcal{G}_o &= \mathcal{L}_o \sqrt{1 - e_o^2}, & \mathcal{H}_o &= \mathcal{G}_o \cos i_o, \\ \ell_o &= M_o, & g_o &= \omega_o, & h_o &= \Omega_o, \end{aligned}$$

where the subscripts i and o indicate the inner and outer orbits, respectively. In these variables, the Hamiltonian up to the first order in $\varepsilon^2 \sim (\frac{\mathcal{L}_i}{\mathcal{L}_o})^4$ can be formally written as

$$\begin{aligned} H &= H(\mathcal{L}_i, \mathcal{G}_i, \mathcal{L}_o, \mathcal{G}_o, \ell_i, g_i, \ell_o, g_o, \mathcal{H}_i + \mathcal{H}_o, h_o - h_i) \\ &\approx H_{0i} + H_{0o} + H_1 \\ &\equiv -\frac{\beta_i}{2\mathcal{L}_i^2} - \frac{\beta_o}{2\mathcal{L}_o^2} + \frac{\beta_1}{2\mathcal{L}_o^2} \frac{(1 - e_i \cos E_i)^2}{(1 - e_o \cos E_o)^3} (1 - 3\Phi^2) \left(\frac{\mathcal{L}_i}{\mathcal{L}_o}\right)^4, \end{aligned} \quad (1)$$

where $\Phi = \Phi(\mathcal{L}_i, \mathcal{G}_i, \mathcal{L}_o, \mathcal{G}_o, \ell_i, g_i, \ell_o, g_o, \mathcal{H}_i + \mathcal{H}_o, h_o - h_i) = \frac{\mathbf{r} \cdot \mathbf{R}}{rR}$, $E_i = E_i(\mathcal{L}_i, \mathcal{G}_i; \ell_i)$ and $E_o = E_o(\mathcal{L}_o, \mathcal{G}_o; \ell_o)$ are the eccentric anomalies of the inner and outer orbits, respectively.

In eq.(1), $\mathcal{H}_o + \mathcal{H}_i$ and $h_o - h_i$ are understood as two single canonical variables conjugating respectively to the negligible h_i and \mathcal{H}_o . And so, they are constants that can be calculated from the initial conditions. The standard way to calculate the two negligible variables is by quadrature, after all the other degrees of freedom are integrated. But in the present context, we have as consequences of the integral of angular momentum

$$\mathcal{H}_i + \mathcal{H}_o = C \equiv |C|, \quad h_o - h_i = \pi, \quad \mathcal{H}_o = \frac{C^2 + \mathcal{G}_o^2 - \mathcal{G}_i^2}{2C},$$

Therefore, only h_i needs to be calculated by quadrature. Because of the short-period terms in the integrand, the numerical quadrature is time-consuming. It is then preferable not to follow the standard way and decouple only $(\mathcal{H}_o, h_o - h_i)$ from the other degrees of freedom at this stage.

For the system defined by the Hamiltonian eq.(1) with $h_o - h_i = \pi$, a first-order integrable system can be achieved by the Von Zeipel transformation (e.g. Harrington 1968, 1969, Marchal 1978, 1990). In

the resulting canonical variables $(\mathcal{L}_I, \mathcal{G}_I, \mathcal{L}_O, \mathcal{G}_O, C; \ell_I, g_I, \ell_O, g_O, h_I)$, called long-period Delaunay variables, the new Hamiltonian can be written as

$$\begin{aligned}\hat{H} &= \hat{H}(\mathcal{L}_I, \mathcal{G}_I, \mathcal{L}_O, \mathcal{G}_O, C, g_I) \\ &= \hat{H}_{0I} + \hat{H}_{0O} + \hat{H}_1 \\ &\equiv -\frac{\beta_i}{2\mathcal{L}_I^2} - \frac{\beta_o}{2\mathcal{L}_O^2} + \frac{\beta_1(3z-5)\mathcal{L}_O}{8\mathcal{G}_O^3} \left(\frac{\mathcal{L}_I}{\mathcal{L}_O}\right)^4,\end{aligned}\quad (2)$$

where

$$z = \frac{\mathcal{G}_I^2}{\mathcal{L}_I^2} \left[2 - \left(\frac{C^2 - \mathcal{G}_I^2 - \mathcal{G}_O^2}{2\mathcal{G}_I\mathcal{G}_O} \right)^2 \right] + 5 \left(1 - \frac{\mathcal{G}_I^2}{\mathcal{L}_I^2} \right) \left[1 - \left(\frac{C^2 - \mathcal{G}_I^2 - \mathcal{G}_O^2}{2\mathcal{G}_I\mathcal{G}_O} \right)^2 \right] \sin^2 g_I. \quad (3)$$

In this time-independent Hamiltonian of five degrees of freedom, there are four negligible variables ℓ_I, ℓ_O, g_O, h_I . Their conjugate variables $\mathcal{L}_I, \mathcal{L}_O, \mathcal{G}_O$ and C , together with the total energy \hat{H} and $z = z(\hat{H}, \mathcal{L}_I, \mathcal{L}_O, \mathcal{G}_O)$ as given by solving eq.(2), are constants known from initial conditions. This confirms the integrability of the transformed Hamiltonian system.

The differential equations for \mathcal{G}_I and g_I , the variables of the only non-negligible degree of freedom, can be integrated simultaneously. But to be more efficient, we first integrate the equation for \mathcal{G}_I , decoupled from g_I by using eq.(3). In terms of $x = \frac{\mathcal{G}_I^2}{\mathcal{L}_I^2} \in (0, 1)$, this equation writes

$$\dot{x} = \pm \frac{3}{2} \frac{\beta_1 \mathcal{L}_I^4}{\mathcal{L}_O^3 \mathcal{G}_O^3} \sqrt{P_1(x)P_2(x)}, \quad (4)$$

where, with $A = \frac{C^2 - \mathcal{G}_O^2}{2\mathcal{G}_O\mathcal{L}_I}$ and $B = \frac{\mathcal{L}_I}{2\mathcal{G}_O}$,

$$\begin{aligned}P_1(x) &= B^2 x^2 - 2(1 + AB)x + z + A^2, \\ P_2(x) &= 4B^2 x^3 - (5B^2 + 8AB + 3)x^2 + (4A^2 + 10AB - z + 5)x - 5A^2.\end{aligned}$$

From the necessary condition $P_1(x)P_2(x) \geq 0$, Marchal (1990) pointed out that x oscillates between two neighbouring roots, $x_a \in (0, 1)$ and $x_b \in (x_a, 1)$, of $P_1(x)P_2(x)$. To be specific, the function $\dot{x}(t)$ defined in eq.(4) changes its sign from negative to positive at x_a , and the opposite is true at x_b .

The difficulty in integrating eq.(4) caused by this unfavorable feature of the right-hand side can be avoided. For this, we introduce a continuously changing angular variable θ , for which $\text{mod}(2\pi)$ is not allowed, by the following variable substitution $x = x_a + (x_b - x_a) \sin^2 \theta$.

Let $\sigma_3, \sigma_4, \sigma_5$ be the other three roots of $P_1(x)P_2(x)$. We have

$$\frac{d\tau}{d\theta} = \mathcal{I}_1(\theta) \equiv \frac{1}{\sqrt{1 - c_1 \sin^2(\theta) + c_2 \sin^4(\theta) - c_3 \sin^6(\theta)}}, \quad (5)$$

where

$$\begin{aligned}\tau &= \frac{3}{4} \frac{\beta_1 \mathcal{L}_I^4}{\mathcal{L}_O^3 \mathcal{G}_O^4} B \sigma \cdot t, \quad \sigma = \sqrt{(\sigma_3 - x_a)(\sigma_4 - x_a)(\sigma_5 - x_a)} > 0, \\ c_1 &= d_1 + d_2 + d_3, \quad c_2 = d_1 d_2 + d_1 d_3 + d_2 d_3, \\ c_3 &= d_1 d_2 d_3 > 0, \quad d_j = \frac{x_b - x_a}{\sigma_{j+2} - x_a}, (j = 1, 2, 3).\end{aligned}$$

Given the initial condition (t_0, θ_0) , the value of θ at any time t can be obtained from an iterative method. And, given θ , $\mathcal{G}_I(> 0)$ can be calculated from the defining formulae of θ and x .

As $|\sin g_I(t)|$ can be solved from eq.(3), the key to determining g_I is its quadrant. Let n be the biggest integer no greater than $2\theta/\pi$. The quadrant of $g_I(t)$ can be deduced from the type of motion, $g_I(0)$ and θ . Depending on the initial conditions, there are three types of motion.

Type 1: $P_2(x_a) = 0$ and $P_2(x_b) = 0$. In this type of motion, g_I oscillates around $\frac{\pi}{2}$ or $-\frac{\pi}{2}$ periodically. In the case of $\sin(g_I(0)) > 0$, $g_I(t)$ is in the first quadrant if n is odd and the second quadrant if n is even. In the other case, $g_I(t)$ is in the third quadrant if n is odd and the fourth quadrant if n is even.

Type 2: $P_2(x_a) = 0$ and $P_1(x_b) = 0$. In this case, g_I always increases as time grows. The $g_I(t)$ is in the same quadrant as $[\hat{\theta}_n, \hat{\theta}_n + \frac{\pi}{2})$, where $\hat{\theta}_n = \frac{(n-1)\pi}{2}$ if $g_I(0)$ is in the same quadrant as $[-\frac{\pi}{2}, \frac{\pi}{2})$, and $\hat{\theta}_n = \frac{(n+1)\pi}{2}$ if $g_I(0)$ is in the same quadrant as $[\frac{\pi}{2}, \frac{3\pi}{2})$.

Type 3: $P_1(x_a) = 0$ and $P_2(x_b) = 0$. The g_I always decreases as time goes by. The $g_I(t)$ is in the same quadrant as $(\hat{\theta}_n - \frac{\pi}{2}, \hat{\theta}_n]$, where $\hat{\theta}_n = (1 - \frac{n}{2})\pi$ if $g_I(0)$ is in the same quadrant as $(0, \pi]$, and $\hat{\theta}_n = -\frac{n\pi}{2}$ if $g_I(0)$ is in the same quadrant as $(-\pi, 0]$.

The other four angular variables can be obtained by quadrature,

$$\begin{aligned} \ell_I(t) &= \ell_I(0) + \frac{\beta_i}{\mathcal{L}_3^3} t + \int_{\theta_0}^{\theta} F_1(x(\vartheta)) \mathcal{I}_1(\vartheta) d\vartheta, & \ell_O(t) &= \ell_O(0) + \frac{\beta_o}{\mathcal{L}_3^3} t + \frac{3}{8} \frac{\beta_1 \mathcal{L}_4^4}{\mathcal{L}_O^4 \mathcal{G}_O^3} (5 - 3z)t, \\ g_O(t) &= g_O(0) + \int_{\theta_0}^{\theta} F_2(x(\vartheta)) \mathcal{I}_1(\vartheta) d\vartheta, & h_I(t) &= h_I(0) + \int_{\theta_0}^{\theta} F_3(x(\vartheta)) \mathcal{I}_1(\vartheta) d\vartheta, \end{aligned}$$

where

$$\begin{aligned} F_1(x) &= \frac{1}{B^2 \sigma} \left[\left(z - \frac{5}{3} \right) + \frac{x(z-2) + (A-Bx)^2}{2(1-x)} \right], \\ F_2(x) &= \frac{5-3z}{2B\sigma} + \frac{1}{2B^2\sigma} \frac{(z-x)(A-Bx)}{x-(A-Bx)^2} [1 + 2B(A-Bx)], \\ F_3(x) &= -\frac{1}{2B^2\sigma} \frac{C}{\mathcal{G}_O} \frac{(z-x)(A-Bx)}{x-(A-Bx)^2}. \end{aligned}$$

If the first-order long-period solution is gotten, one can make inverse transformations of the solution to the original coordinate system.

3 COMPARISON BETWEEN M-MODEL AND K-MODEL

In order to compare the accuracy of different models in calculating the observational quantities, it is necessary to do a numerical experiment. For the time being, we are interested in only the systems with negligible 2nd-order perturbations. Therefore we generated 1000 systems, which satisfy $|H_2|/|H_{0i} + H_{0o} + H_1| < 0.01$ in $[-100, 100]$ years, and H_2 is the second-order perturbation term in the Hamiltonian (1). This time span is used because the practical cycle of a star catalog is usually less than one hundred years. As expected, for some of the generated systems, especially for the systems with large periods and high eccentricities of the outer orbits, the first-order averaged perturbations are too large. For such a case, M-model fails to be the first-order model. We just consider the samples that satisfy

$$|H_1/H_{0i}| < 0.1, \quad |H_1/H_{0o}| < 0.5, \quad (6)$$

during $[-P_t, P_t]$ years, where $P_t \geq \max(100, P_o)$, and P_o represents the initial period of the outer orbit. Nearly 90 samples are excluded by condition eq.(6). In addition, Delaunay elements are not effective in describing the orbits that are near circular, near parabolic or near the reference plane, and M-model is not suitable to be used in coplanar motion. If there are very small divisors, the implicit Zeipel transformations can not be solved by the iterative method. Another ~ 40 samples are excluded, and 870 samples remain. The remnant samples are used to do a numerical experiment to check the accuracy of M-model compared with K-model.

We calculate the positions of three bodies in the center-of-mass frame during the $[-100, 100]$ years by M-model and K-model, respectively. As a comparison standard, these positions are also calculated by the numerical solution (*N-model* for short). Denote the root-mean-squared errors (RMSE) of the 9-dimensional vectors of M-model relative to those of N-model by d_M , and the RMSE of the 9-dimensional vectors of K-model relative to those of N-model by d_K . When $(r/R)^3 \ll (m_1 + m_2)/m_t$, generally $d_M/d_K \ll 1$, as is shown in Fig. 1. Fig. 1 shows that M-model is apparently better than K-model in accuracy when the abscissa is smaller than -1.4 . When the abscissa is greater than -1.4 , Fig. 1 reveals that for most samples the M-model is still more accurate than K-model.

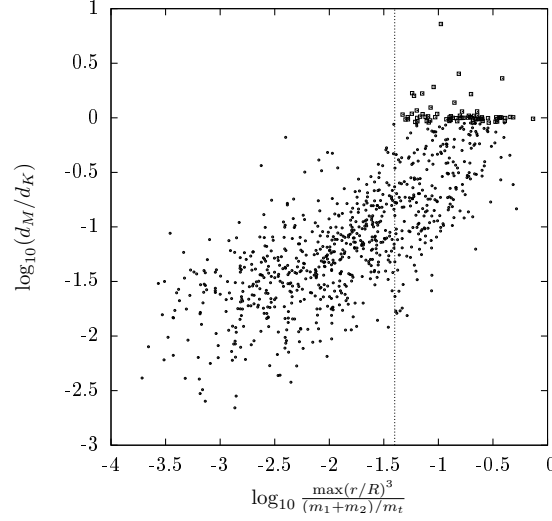


Fig. 1 The abscissas on the x-axis are calculated in $[-P_t, P_t]$ years. The abscissa of the dashed line is -1.4 . Circular points represent the samples that satisfy $d_M/d_K < 0.9$, while square points represent the samples that satisfy $d_M/d_K \geq 0.9$. There are 798 circular points and 72 square points.

For a few samples which are at the up-right quarter of Fig. 1, the accuracy of M-model is not as good as that of K-model. The phenomena can be explained by the perturbations and the improper use of the Delaunay elements.

There is one sample whose ordinate is apparently greater than 0.5 in Fig. 1. We found that the outer orbit of this sample has a very large period and high eccentric. The $\max \frac{(r/R)^3}{(m_1+m_2)/m_t}$ is really small during the considered $[-100, 100]$ years, and K-model is very approximate to N-model. While M-model considers the averaged perturbations which are much greater. We calculated $\max |H - \hat{H}_{0i} - \hat{H}_{0o} - \hat{H}_1|$ in $[-P_t, P_t]$ years and $\max |H - H_{0i} - H_{0o}|$ in $[-100, 100]$ years. The former is more than 1000 times of the latter, and this supports that M-model is not a first-order model in such cases.

As the abscissas of samples represented by squared points are not sufficiently small (bigger than -1.4), the inaccuracies caused by small divisors cannot be ignored. For some samples represented by squared points in Fig. 1, the detailed reasons are complex and uncertain currently. In all, M-model is better than K-model in accuracy for $\sim 80\%$ of the samples, and can be credibly applied when the abscissa is smaller than -1.4 .

4 THE APPLICATION

Simplifications of M-model can be made according to the results of the numerical experiment. In eq.(5), $x(\theta(t))$ can be solved efficiently by an approximation. Generally $\mathcal{I}_1(\vartheta)$ can be written

$$\mathcal{I}_1(\vartheta) = \mathcal{I}_2(\vartheta) + [\mathcal{I}_1(\vartheta) - \mathcal{I}_2(\vartheta)], \quad (7)$$

where $\mathcal{I}_2(\vartheta)$ can be defined as

$$\mathcal{I}_2(\vartheta) = \begin{cases} \frac{1}{\sqrt{1-c_1 \sin^2 \vartheta + c_2 \sin^4 \vartheta}}, & \text{if } c_1^2 - 4c_2 > 0, 1 - c_1 + c_2 \gg c_3 > 0, c_2 > 0, \\ \frac{1}{\sqrt{1-c_1 \sin^2 \vartheta}}, & \text{if } c_1^2 - 4c_2 \leq 0, 1 - c_1 \gg |c_2 - c_3| > 0, \end{cases}$$

Table 1 The application results of the 25 observed triple stars during the time span from 1900.0 to 2100.0.

system name (WDS)	perturbation order ($\log_{10} \frac{\max[(r/R)^3]m_t}{m_1+m_2}$)	d_M (AU)	d_{MC} (AU)	d_K (AU)	Improvement ($\log_{10} \frac{d_{MC}}{d_K}$)	Type (1/2)
00325+6714	-1.52	2.77E-2	2.78E-2	0.47	-1.23	2
01148+6056	-4.64	6.11E-7	4.96E-4	1.96E-3	-0.59	1
02022+3643	-1.56	0.013	0.013	0.23	-1.25	1
03082+4057	-4.36	7.05E-4	1.43E-2	8.32E-2	-0.76	2
04142+2812	-4.13	4.78E-5	1.10E-4	0.10	-2.96	1
04400+5328	-1.53	0.119	0.119	0.96	-0.91	2
06262+1845	-7.69	2.13E-7	2.63E-6	6.01E-5	-1.36	2
07201+2159	-7.35	7.71E-9	7.58E-7	1.23E-5	-1.21	2
10373-4814	-2.88	2.60E-4	2.41E-3	2.72E-2	-1.05	2
10373-4814	-2.77	3.49E-4	4.73E-3	3.60E-2	-0.88	2
11308+4117	-6.22	1.23E-7	4.96E-6	4.06E-4	-1.91	2
12108+3953	-1.64	0.180	0.180	0.99	-0.74	2
12199-0040	-3.24	1.31E-3	3.26E-3	0.18	-1.74	2
15183+2650	-1.76	0.014	0.014	0.12	-0.93	2
16578+4722	-2.39	6.97E-4	8.63E-4	1.66E-3	-0.28	2
17539-3445	-7.14	4.58E-7	2.47E-5	9.87E-5	-0.60	2
19155-2515	-4.08	2.06E-5	2.03E-4	1.89E-2	-1.97	1
20396+0458	-1.45	7.17E-2	7.17E-2	1.30	-1.26	1
20475+3629	-2.15	1.19E-3	1.19E-3	5.27E-2	-1.65	2
22038+6437	-5.52	4.26E-7	4.91E-5	1.40E-4	-0.46	2
22288-0001	-4.03	2.95E-4	3.32E-4	2.44E-2	-1.87	2
22388+4419	-1.86	1.94E-2	1.94E-2	0.77	-1.60	2
23078+7523	-3.98	8.76E-6	1.18E-5	2.08E-3	-2.25	2
23393+4543	-1.77	5.05E-2	5.08E-2	0.72	-1.15	2
23393+4543	-1.86	5.53E-2	5.53E-2	0.45	-0.91	2

The formulas for calculating $\int_0^\theta \mathcal{I}_2(\vartheta) d\vartheta$ by elliptic functions can refer to Byrd & Friedman (1971). Similar studies which used elliptic functions can refer to Kozai (1962), Söderhjelm (1982) and Solovaya (2003). The remainder term $\mathcal{I}_1(\vartheta) - \mathcal{I}_2(\vartheta)$ is generally small and sometimes can be ignored. If $\mathcal{I}_1(\vartheta) - \mathcal{I}_2(\vartheta)$ can be ignored, θ can be calculated analytically by elliptic functions. But here $\int_{\theta_0}^\theta [\mathcal{I}_1(\vartheta) - \mathcal{I}_2(\vartheta)] d\vartheta$ is considered by simple Newton-Cotes integration formula to make a better approximation. θ can be solved approximately by an iterative method. The three angular variables ℓ_I, g_O, h_I can be integrated also by simple Newton-Cotes integration formula simultaneously. Another simplification is that the implicit Zeipel transformations from the averaged variables to the osculating elements can be turned into explicit. We call this model as *MC-model*.

We now apply this model to 25 real triple stars with determined dynamical state (component masses and kinematic parameters). The results are listed in Table 1 including system name, order of magnitude of the perturbation ($\log_{10} \frac{\max[(r/R)^3]m_t}{m_1+m_2}$), the RMSEs of M-model, K-model and MC-model, the ratio of the RMSE of MC-model to that of K-model ($\log_{10} \frac{d_{MC}}{d_K}$) and the type of motion. According to this table, the accuracy between M-model and MC-model is comparable. For all these stars, the RMSE of MC-model in comparison with the K-model's, is reduced significantly. Indeed, for $\sim 60\%$ stars, the RMSEs are reduced by more than one order of magnitude. To show more details, we take WDS 02022+3643 as an example. From the N-model, the deviations of component positions calculated by M-model, MC-model and K-model, respectively, are shown in Fig. 2. From this figure, we know that the performance of MC-model is almost as good as M-model's. When compared with K-model, the model accuracy is significantly improved and the applicable time span is significantly increased.

As we all know, one of the important factors decide the quality of dynamical state determination is the accuracy of the dynamical model. In order to show the improvement in this respect brought by the high accuracy MC-model, we apply both this model and K-model to two systems, WDS 20396+0458 (HIP 101955, type 1) and WDS 00325+6714 (HIP 2552, type 2).

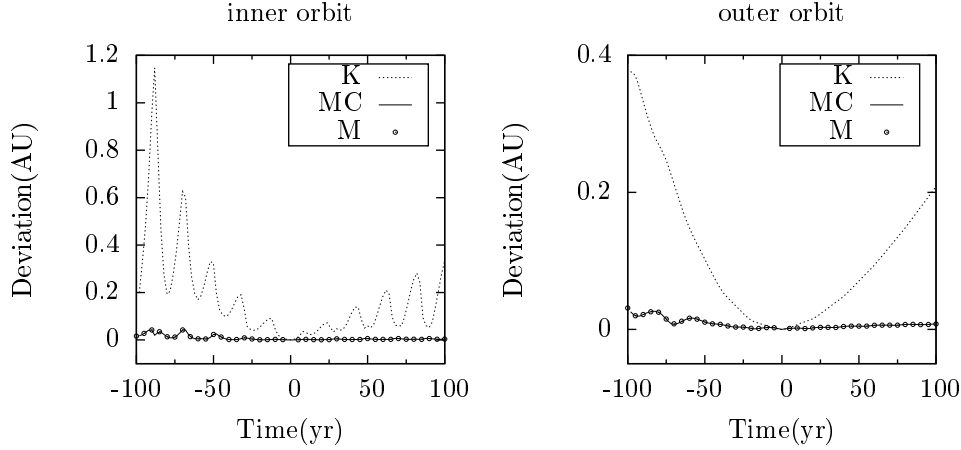


Fig. 2 From the N-model, the deviations of component positions of WDS 02022+3643 calculated by using M-model, MC-model and K-model, respectively.

Two kinds of observations, relative position data (RPD) and the Hipparcos Intermediate Astrometric Data (HIAD) are used in the fitting. RPD are extracted from the Washington Double Star (WDS) Catalog (Mason et al. 2001), and the Fourth Catalog of Interferometric Measurements of Binary Stars (Hartkopf et al. 2001). HIAD are the abscissa residuals with respect to a reference point, the abscissa of which is calculated from a given solution. HIAD are read from the resrec folder on the catalogue DVD of Leeuwen(2007). With these observational data, the maximum likelihood estimate of model parameters is obtained by minimizing the objective function (χ^2)

$$\chi^2 \equiv \sum_{i=1}^N \left(\frac{y_i - y(x_i; a_1 \cdots a_M)}{\sigma_i} \right)^2, \quad (8)$$

where y_i is the observational quantity, $y(x_i; a_1 \cdots a_M)$ is the corresponding calculated value according to the model parameters $a_1 \cdots a_M$. We use the Bounded Variable Least Squares (BVLS) algorithm (Lawson & Hanson 1995) to minimize the χ^2 .

HIP 101955 is a nearby low-mass triple star. There are 15 RPD points spanning from 1998 to 2008 of inner orbit, 46 points from 1934 to 2008 of the outer one, and 91 HIAD in reference to a solution with 5 parameters. In the previous determinations of the dynamical state, the Kepler's two-body motion model is applied separately to the inner $\{Aa, Ab\}$ and the outer $\{Am, B\}$ where Am is the center-of-mass of the inner binary AaAb (Malogolovets et al. 2007). The results are collected in the *Sixth Catalog of Orbits of Visual Binary Stars*(ORB6) (Hartkopf & Mason 2014), where the inner and outer orbits are roughly evaluated as good and reliable, respectively, according to the orbital coverage of the observations. Because more observations are added, we firstly also use the K-model to fit observations. In comparison with the previous results, the χ^2 is found to be reduced by $\sim 66\%$. When the fitting model is replaced by MC-model, the χ^2 is further reduced by $\sim 44\%$. Therefore, we conclude that using high accuracy MC-model, the fitting result is significantly better than the previous K-model's results. Using the

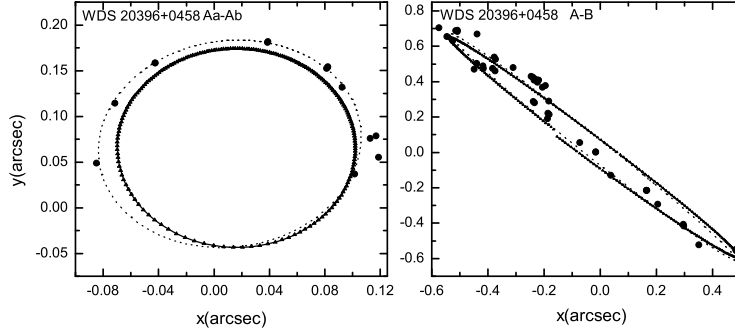


Fig. 3 The fitting result of HIP 101955.

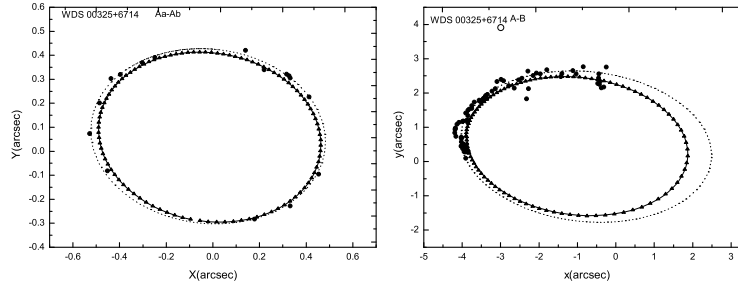


Fig. 4 The fitting result of HIP 2552. The open circle is a discarded point.

fitted dynamical state parameters, the RMSEs of MC-model and K-model are calculated during the forward 100 years, that is, from 2008 to 2108. The RMSE of MC-model in comparison with the K-model's, is significantly reduced by more than 80%, from 35.9mas (K-model) to ~ 6.0 mas (MC-model). This result shows that though starting with the same initial condition, for HIP 101955, the K-model can not be used to predict the component positions.

For HIP 2552, there are 16 RPD points spanning from 1989 to 2005 of inner orbit, 75 points from 1923 to 2010 of the outer one, and 151 HIAD in reference to an acceleration solution with 7 parameters. The inner and outer orbits were provided by Docobo et al. (2008) and are evaluated as good and indeterminate by ORB6. K-model is also firstly used to fit the observations. In comparison with the previous fitting results, the χ^2 is reduced by $\sim 42\%$. When the fitting model is replaced by MC-model, though the χ^2 is not significantly reduced, the RMSE is reduced from 10.5mas which is calculated by K-model to 0.74mas by MC-model. Using the fitted dynamical parameters, during the forward 100 years, the RMSE of K-model is 29.8mas while ~ 5.0 mas of MC-model. Therefore, K-model is also not suitable to predict the component positions for HIP 2552.

We plot the fitted trajectories of HIP 101955 and HIP 2552, respectively, in Fig. 3 and Fig. 4. In these two figures, the filled circles are the RPD used in fitting, solid curves represent the previous double two-body model while the dotted curves are the fitted trajectories calculated using the MC-model. The trigonometric curves represent the N-model. As shown in the two figures, the difference between MC-model and the N-model is small enough to be ignored. The fitted dynamical state parameters and their 1σ errors are listed in Table 2 and 3.

Table 2 The fitted dynamical masses and kinematic parameters of HIP 101955.

parameter				unit
M	0.786 ± 0.11	0.493 ± 0.11	0.516 ± 0.21	M_{\odot}
r_{Ab}	-0.0598 ± 0.0050	0.127 ± 0.0050	-0.0188 ± 0.022	arcsec
r_B	-0.188 ± 0.0040	0.173 ± 0.0038	0.902 ± 0.025	arcsec
v_{Ab}	-0.102 ± 0.0062	-0.206 ± 0.016	0.111 ± 0.039	arcsec/yr
v_B	0.0367 ± 0.0027	-0.174 ± 0.0066	0.0669 ± 0.016	arcsec/yr

Table 3 The fitted dynamical masses and kinematic parameters of HIP 2552.

parameter				unit
M	0.389 ± 0.038	0.0969 ± 0.038	0.177 ± 0.212	M_{\odot}
r_{Ab}	-0.0614 ± 0.047	-0.298 ± 0.029	0.290 ± 0.032	arcsec
r_B	-4.029 ± 0.016	0.609 ± 0.015	-0.318 ± 1.8	arcsec
v_{Ab}	0.235 ± 0.015	-0.0331 ± 0.013	0.000668 ± 0.025	arcsec/yr
v_B	0.0478 ± 0.0059	-0.0556 ± 0.0029	0.0455 ± 0.0097	arcsec/yr

5 CONCLUSION AND DISCUSSION

Marchal's first-order analytical solution is implemented and a more efficient simplified version is applied to real hierarchical triple stars. The results show that the proposed first-order model is preferable to the classical double two-body model both in fitting observational data and in predicting component positions.

As pointed out in section 3, there are a few cases to which the M-model doesn't apply, because of the inadequacy of the Delaunay elements. For these cases, Poincaré elements should be used instead. There are also a few cases when the first-order perturbations are very small in the time span of observations, but its maximum value over the whole period of the outer orbit is too large to apply M-model. For these cases, our preliminary studies show that it is possible to give a suitable first-order solution without resorting to averaging over the outer orbit.

Acknowledgements The authors would like to thank the reviewers of this paper for their comments and suggestions, and also thanks to the editors of this journal. This research is supported by the National Natural Science Foundation of China under Grant Nos. 11178006 and 11203086.

References

- Aarseth S.J., 2003, Gravitational N-Body Simulations, (Cambridge :Cambridge University Press)
- Binney, J., & Merrifield, M., 1998, Galactic Astronomy, (Princeton, NJ:Princeton University Press)
- Byrd P.F., & Friedman M.D., 1971, Handbook of elliptic integrals for engineers and scientists, (2nd ed.; Berlin: Springer-Verlag Berlin)
- Docobo, J. A., Tamazian, V. S., Balega, Y. Y., et al., 2008, A&A, 478, 187
- Harrington R.S., 1968, AJ, 73, 190
- Harrington R.S., 1969, Celestial Mechanics, 1, 200
- Hartkopf, W. I., Mason, B. D., & Worley, C. E., 2001, AJ, 122, 3472
- Hartkopf, W. I., & Mason, B. D., Sixth Catalog of Orbits of Visual Binary Stars,
<http://ad.usno.navy.mil/wds/orb6.html>
- Kozai Y., 1962, AJ, 67, 591
- Lawson, C.L. & Hanson R.J. ed. 1995, Solving Least Squares Problems, (2nd ed.; Philadelphia: SIAM)

- Li P.J., Fu Y.N., & Sun Y.S., 2009, *A&A*, 504, 277
- Liu H.D., Ren S.L., Xia F. et al., 2009, *Acta Astronomica Sinica*, 50, 312
- Malogolovets, E. V., Balega, Yu. Yu. & Rastegaev, D. A., 2007, *Astrophysical Bulletin*, 62, 111
- Marchal C., Bozis G., 1982, *Celestial Mechanics*, 26, 311
- Marchal C., 1978, *Acta Astronautica*, 5, 745
- Marchal C., 1990, *The Three-Body Problem*, (Amsterdam: Elsevier Science Publishers B.V.)
- Mason, B. D., Wycoff, G. L., Hartkopf, W. I., Douglass, G. G., & Worley, C. E., 2001, *AJ*, 122, 3466
- Orlov V. V., & Zhuchkov R. Ya., 2005, *Astronomy Reports* 49, 201
- Söderhjelm S., 1982, *A&A*, 107, 54
- Solovaya N.A., 2003, *Contrib. Astron. Obs. Skalnaté Pleso*, 33, 179
- Tokovinin A. A., 1997, *A&AS*, 124, 75
- Urban S.E., & Seidelmann P.K., 2014, *Explanatory supplement to the astronomical almanac*, (3rd ed.; Mill Valley: University Science Books) 531
- Valtonen M., & Karttunen H., 2006, *The three-body problem*, (Cambridge: Cambridge University Press)
- van Leeuwen, F., 2007, *Hipparcos, the New Reduction of the Raw Data*, *Astrophysics and Space Science Library*, 350, eds., F. van Leeuwen, (Berlin: Springer)